

Figure 1. Red-violet ratio mosaics of Viking Orbiter 1 images of the map area, taken almost a Mars year after the images used to create the photomosaic base map. White corresponds to red/violet<2.2, totally black regions indicate no image coverage or red/violet < 1.5. Polar stereographic projection (same as map base); map outline shown, north is up. Area shown in each mosaic ~310 km across. **A.** Rev 720 mosaic ($L_p=100^\circ$), taken during a period of hazy atmospheric conditions. **B.** Rev 768 mosaic ($L_p=119^\circ$), showing much clearer atmospheric conditions and changes in frost distribution.

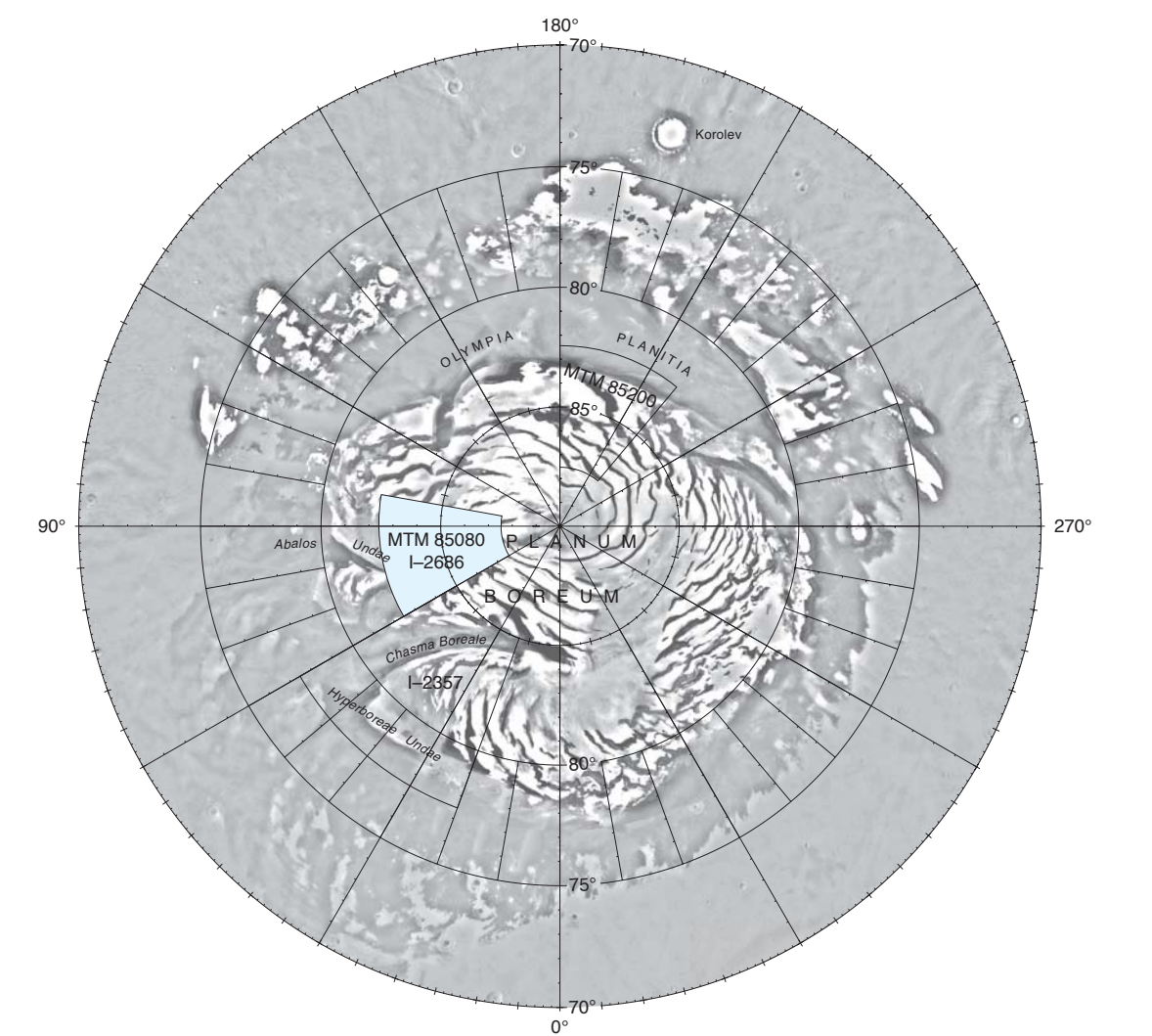


Figure 2. Index map showing major physiographic features and 1:500,000-scale maps in Planum Boreale region completed or in progress in Mars Geologic Mapping Program. Mars Transverse Mercator (MTM) numbers indicate latitude and longitude of center of maps. I-number indicates published U.S. Geological Survey map.

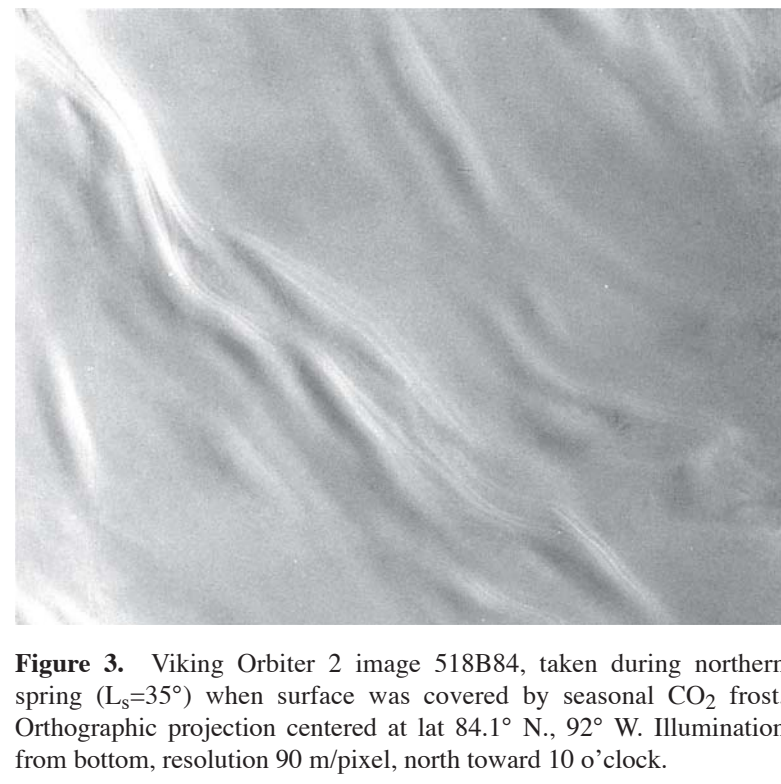


Figure 3. Viking Orbiter 2 image 518B84, taken during northern spring ($L_p=35^\circ$) when surface was covered by seasonal CO_2 frost. Orthographic projection centered at lat 84.1° N, 92° W. Illumination from bottom, resolution 90 m/pixel, north toward 10 o'clock.

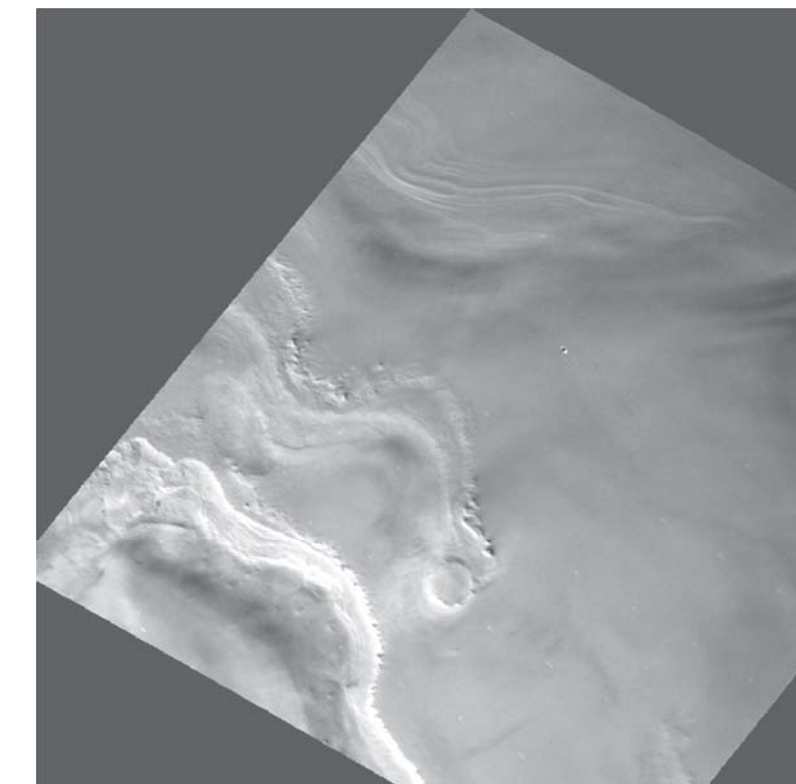


Figure 4. Viking Orbiter 2 image 560B43, taken during northern spring ($L_p=54^\circ$) when surface was covered by seasonal CO_2 cap. Polar stereographic projection (same as map base), illumination from lower left, north is up, image ~60 km across. Bright ringdark spot slightly above and right of center is an artifact of the camera system.

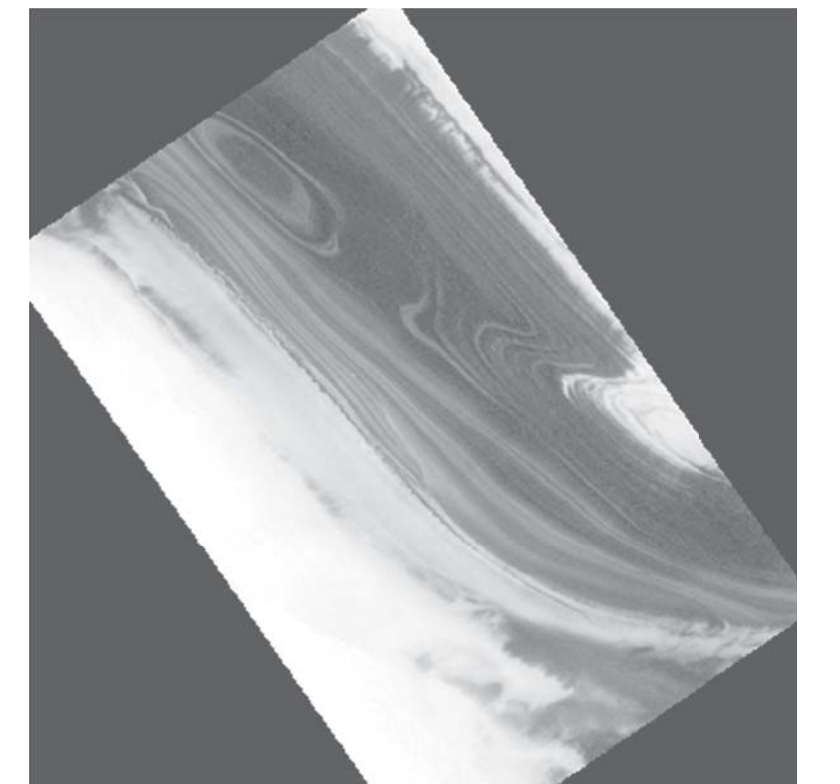
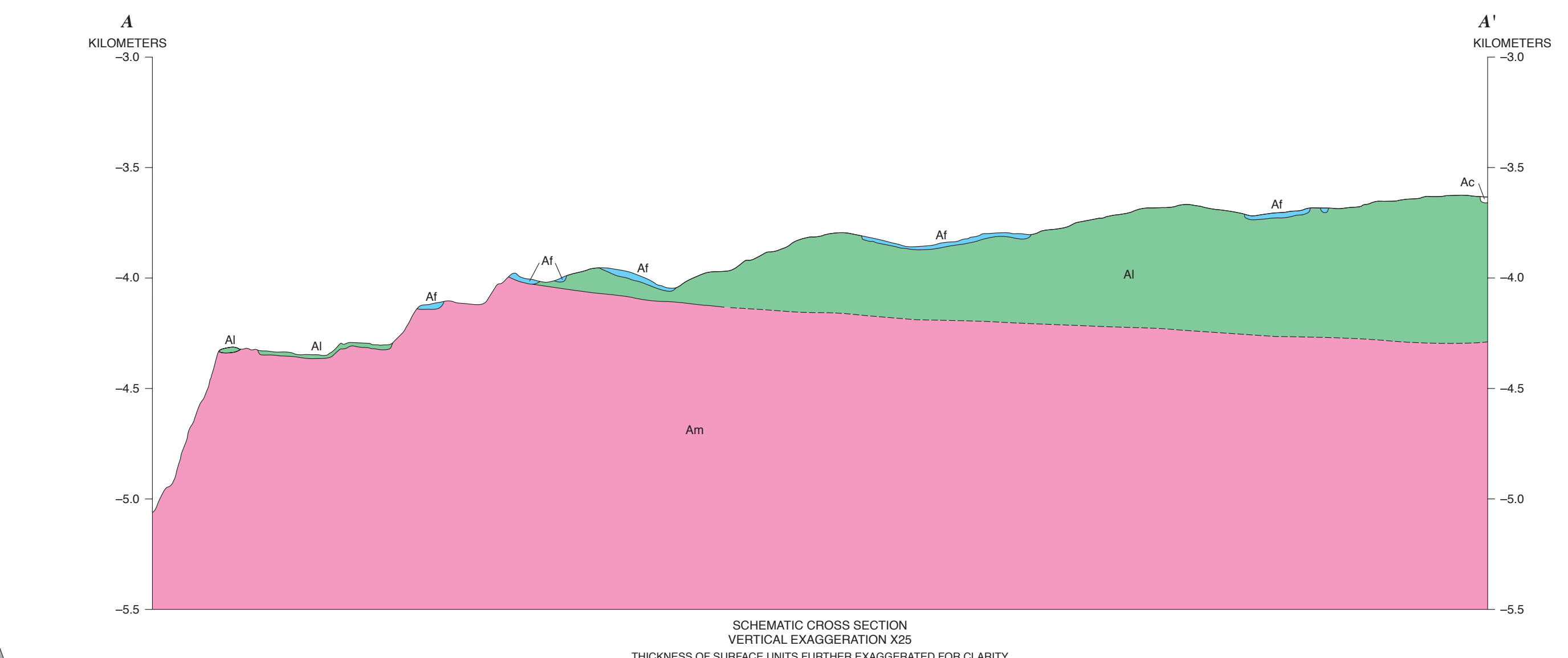


Figure 5. Part of Viking Orbiter 2 image 60B42, taken during northern summer ($L_p=135^\circ$), showing angular unconformity at center. Polar stereographic projection (same as map base), illumination from lower left, north is up, image ~23 km across.



extent of the north polar cap appeared the same during the Mariner 9 and Viking Missions (Bass and others, 2000), which suggests that it is controlled by underlying topography. Albedo patterns in these summertime images are correlated with topographic features seen in springtime images (fig. 3). Areas of the highest albedo must be covered by nearly pure coarse-grained ice or dusty fine-grained frost (Clark and Lucy, 1984; Kieffer, 1999). The presence of perennial frost is thought to aid in the long-term retention of dust deposits (James and others, 1979), so areas covered by frost all year are the most likely sites of layered deposit formation.

GEOLOGIC PROCESSES AND HISTORY

The polar layered deposits appear to have formed through deposition of water ice and dust, modulated by global climate changes during the last few million to hundreds of million years (Murray and others, 1972; Cuts, 1973; Soderholm and others, 1973; Carr and others, 1979; Squires, 1979; Toon and others, 1980; Carr, 1982; Howard and others, 1982; Pollack and Toon, 1982; Platt and others, 1988). However, the details of the relation between the variations of Mars' orbit and axis and geologic observations are not clear (Thomas and others, 1992). In particular, the apparent contrast in ages of the north and south polar layered deposits, as indicated by their different crater densities (Cuts and others, 1976; Platt and others, 1988; Herkenhoff and Platt, 2000), is paradoxical. The geology of this quadrangle illustrates some of the processes that are important in the evolution of the northern deposits.

The contact relations between the layered deposits (unit Ai) and the mantle material (unit Am) seen in this and nearby quadrangles indicate that the layered deposits postdate the mantle material. With the exception of areas covered by the polar ice cap (unit Ac), the north polar layered deposits appear to have undergone net erosion in the recent geologic past, as strata are exposed in many places. The layered deposits have likely accumulated recently in areas covered by the polar ice cap, but deposition rates are poorly constrained. Similarly, rates of erosion cannot be accurately determined, but on the basis of the lack of preserved impact craters, resurfacing rates appear to be at least 2.3 mm/yr (Herkenhoff and Platt, 2000). The partly buried crater shown in figure 4 was likely formed in the mantle material (unit Am) before the layered deposits were laid down and has only recently been exhumed.

Solar heating of the exposed layered deposits causes sublimation of the water ice within them (Toon and others, 1980; Hofstadter and Murray, 1990), probably forming a lag deposit of nonvolatile material. Such a nonvolatile layer would protect underlying water ice from further sublimation. Herkenhoff and Murray (1990a) proposed that minor amounts of dark dust exist in the layered deposits along with the bright, red dust mantle that covers much of the martian surface. The dark dust may preferentially form filamentary sublimation residue particles (Storrs and others, 1988) that eventually break free of the surface and saltate, ejecting the remaining dust into suspension. Dark particles 100 μ m in size will continue to saltate until trapped by an obstacle or depression, possibly forming the dunes that surround the north polar layered deposits (Herkenhoff and Vasavada, 1999).

Acknowledgments.—Trent Hare assisted in the processing of MOLA data, and Ana Greco assisted in the processing of Viking Orbiter color mosaics. Reviews of this map by Bob Anderson and Alan Howard were much appreciated. This work was supported by the NASA Planetary Geology and Geophysics Program.

REFERENCES CITED

- Bass, D.S., Herkenhoff, K.E., and Page, D.A., 2000, Variability of Mars' north polar water ice cap I: Analysis of Mariner 9 and Viking Orbiter imaging data, *Iceans*, v. 144, p. 382–396.
Blasius, K.R., Cuts, J.A., and Howard, A.D., 1982, Topography and stratigraphy of martian polar layered deposits, *Iceans*, v. 50, p. 149–160.
Carr, M.H., 1982, Periodic climate change on Mars: Review of evidence and effects on distribution of volatiles, *Iceans*, v. 50, p. 129–139.
Clark, R.N., and Lucy, P.G., 1984, Spectral properties of ice-particle mixtures and implications for remote sensing—1. Intimate mixtures, *Journal of Geophysical Research*, v. 89, p. 6341–6348.
Cuts, J.A., 1973, Nature and origin of layered deposits of the martian polar regions, *Journal of Geophysical Research*, v. 78, p. 4231–4239.
Cuts, J.A., Blasius, K.R., Briggs, G.A., Carr, M.H., Greeley, Ronald, and Masursky, Harold, 1976, North polar region of Mars: Imaging results from Viking 2, *Science*, v. 194, p. 1329–1337.
Cuts, J.A., Blasius, K.R., and Roberts, W.J., 1979, Evolution of martian polar landscapes: Interplay of long-term variations in perennial ice cover and dust storm intensity, *Journal of Geophysical Research*, v. 84, p. 2975–2994.
Dial, A.L., Jr., 1984, Geologic map of the Mare Boreum area of Mars, U.S. Geological Survey Miscellaneous Investigations Series I-1640, scale 1:500,000.
Dial, A.L., Jr., and Dolan, J.M., 1984, Geologic map of Science Station Area 4, Chasma Boreale region of Mars, U.S. Geological Survey Miscellaneous Investigations Series Map I-2357, scale 1:500,000.

ping of the south polar layered deposits (Herkenhoff and Murray, 1992, 1994; Herkenhoff, 1998, 2001).

Published geologic maps of the north polar region of Mars are based on images acquired by Mariner 9 (Scott and Carr, 1978) and the Viking Orbiters (Dial, 1984; Tanaka and Scott, 1987; Dial and Dolan, 1994). The extent of the layered deposits and other units varies among previous maps, in particular within Chasma Boreale. The present map agrees most closely with the map by Dial and Dolan (1994); the mantle material is exposed farther north than mapped by Tanaka and Scott (1987). The polar ice cap, areas of partial frost cover, the layered deposits, and two nonvolatiles surface units—dark mantle and dark material—were mapped in the south polar region by Herkenhoff and Murray (1990a) at 1:2,000,000 scale using a color mosaic of Viking Orbiter images. Viking Orbiter rev. 726, 768, and 771 color mosaics (taken during the northern summer of 1978) were constructed and used to identify similar color/albedo units in the north polar region, including the dark, saltating material that appears to have sources within the layered deposits (Thomas and Weitz, 1989). However, no dark material has been recognized in this map area. No significant difference in color exists between the layered deposits and the mantle material mapped by Dial and Dolan (1994), indicating that they are either composed of the same materials or are both covered by eolian debris (Herkenhoff and Murray, 1990a; Herkenhoff, 1998). Therefore, in this map the color mosaics are most useful for identifying areas of partial frost cover (fig. 1). Because the resolution of the color mosaics is not sufficient to map the color/albedo units in detail at 1:500,000 scale, contacts between them were recognized and mapped using higher resolution black-and-white Viking Orbiter images. The Viking Orbiter 2 images used to construct the map base were taken during the northern summer of 1976 (mostly $L_p=137^\circ$ – 135°), with resolutions typically around 60 m/pixel (U.S. Geological Survey, 1966). As noted on the published base, errors of up to 5 km exist in the placement of images in the base map; such errors are evident upon comparison of sheet 1 (summer) and sheet 2 (spring). Therefore, a new photomosaic base was created during map production and the network was edited to mantle material base.

No craters have been found in the north polar layered deposits or polar ice cap (Cuts and others, 1976; Herkenhoff and Platt, 2000). The observed lack of craters larger than 200 m implies that the surfaces of these units are no more than 100,000 years old or that they have been resurfaced at a rate of at least 2.3 mm/yr. The recent cratering flux on Mars is poorly constrained, so inferred resurfacing rates and ages of surface units are uncertain by at least a factor of 2.

PHYSIOGRAPHIC SETTING

The area of this map lies mostly within Planum Boreale (fig. 2), a plateau about 1,000 km across and up to 3 km high (Zuber and others, 1998; Smith and others, 1999). The plateau is characterized by the smoothly sculptured landforms of the layered deposits, with about 1 km of relief at its perimeter. The boundary of the plateau is near lat 80° N, south of this map area, except at the large reentrant Chasma Boreale. Areas predominantly covered by frost are typically smooth and level (regional slopes < 0.2°), whereas defrosted bands slope 1° to 8° overall (Blasius and others, 1982; Zuber and others, 1999). In many cases, the scarp form low-relief troughs that are asymmetrical in cross section (Zuber and others, 1998). Symmetrical albedo features such as dark bands are often associated with topographic features, as indicated by a comparison of figure 3 and the photomosaic base map area. MOC

images show that layered deposit exposures are rough in appearance and show evidence for deformed beds and unconformities (Malin and Edgett, 2001). No angular unconformities have been mapped within the south polar layered deposits (Herkenhoff and Murray, 1992, 1994; Herkenhoff, 1998, 2001). In contrast, truncated layers have been recognized in higher resolution Viking images of the north polar region (Cuts and others, 1976; Howard and others, 1982). Angular unconformities have been found within this map area—for example, lat 85.7° N, long 61° W, lat 82.6° N, long 82° W (see also figure 8 on p. 776 of Thomas and others, 1992), and lat 83.0° N, long 90° W. The last locale is mapped as a small scarp because of the brightness of the layer just north of the unconformity in image 60B42 (fig. 5), but the brightening may be due to higher albedo (frost) rather than a slope toward the sun. In either case, a layer appears to have been deposited over an exposure of older layers and probably was then eroded to expose the older layers again. This scenario is consistent with previously published interpretations based on similar observations in other parts of the north polar layered deposits (Howard and others, 1982). Angular unconformities are mapped in places at the contact between the layered deposits and the high-albedo units, consistent with the interpretation that the high-albedo units thinly veneer older units in most places.

Structural deformation in this area appears to be minimal or absent, as no faulting or folding has been observed. The scars and troughs in the layered deposits are interpreted as erosional rather than structural features because of the lack of folded or offset layers. Though the angular unconformities could have been caused by faulting, the relations observed (see fig. 3) suggest that they were formed by erosion and deposition without folding or faulting. Future analysis of MOC images of these unconformities may aid in their interpretation.

The partial frost cover (unit A0) is interpreted as a mixture of water frost and defrosted ground on the basis of its albedo, color, and temporal variability. This interpretation is consistent with the Viking observations of relatively high concentrations of water vapor over the north polar cap during summer (Farmer and others, 1976) and with surface temperatures indicative of dirty water ice (Kieffer and others, 1976). Although patches of frost and bare ground can be distinguished in places, the scale of mixing is commonly below the resolution of the images. The variability of albedo in this unit seen in Viking Orbiter summertime images is probably due to varying amounts of partial frost cover. These variations are not mapped, and all are included in unit A0. Many of the boundaries between the partial frost cover and adjacent units are narrowly gradational at the resolution of the images, but they are drawn as solid lines for simplicity. Bass and others (2000) found that frost albedo reaches a minimum early in the northern summer, then increases during the rest of the summer season. This behavior, which is not extensive in the south polar region (Herkenhoff and Murray, 1992, 1994; Herkenhoff, 2001), is evident in figure 1. Areas covered by frost are less red and therefore dark in figure 1 and have become more extensive later in the summer. The increase in albedo is interpreted as resulting from condensation of H_2O from the atmosphere onto cold traps in the north polar region (Bass and others, 2000). Because the images used for the base and for mapping were taken in mid-summer, the extent of the high-albedo units shown on this map is greater than during early summer.

The albedo of the residual polar ice cap (unit Ai) is higher than all other units on this map. The contact with the partial frost cover (unit A0) is gradational in many areas, most likely because unit Ai represents incomplete cover of the same material (H_2O) frost that composites unit A0. The summer

Farmer, C.B., Davis, D.W., and La Porte, D.D., 1976, Mars: Northern summer ice cap-water vapor observations from Viking 2, *Science*, v. 194, p. 1339–1341.
Herkenhoff, K.E., 1998, Geologic map of the MTM-85280 quadrangle, Planum Australe region of Mars, U.S. Geological Survey Miscellaneous Investigations Series I-2595, scale 1:500,000.
—, 2001, Geologic map of the MTM-85000 quadrangle, Planum Australe region of Mars, U.S. Geological Survey Geologic Investigations Series I-2686, scale 1:500,000.
Herkenhoff, K.E., and Murray, B.C., 1990a, Color and albedo of the south polar layered deposits on Mars, *Journal of Geophysical Research*, v. 95, no. B2, p. 1343–1358.
—, 1990b, High resolution topography and albedo of the south polar layered deposits on Mars, *Journal of Geophysical Research*, v. 95, no. B9, p. 14,511–14,522.
—, 1992, Geologic map of the MTM-90000 area, Planum Australe region of Mars, U.S. Geological Survey Miscellaneous Investigations Series I-2304, scale 1:500,000.
—, 1994, Geologic map of the MTM-85000 quadrangle, Planum Australe region of Mars, U.S. Geological Survey Miscellaneous Investigations Series I-2391, scale 1:500,000.
Herkenhoff, K.E., and Platt, J.J., 2000, Surface ages and resurfacing rates of the polar layered deposits on Mars, *Iceans*, v. 144, p. 245–253.
Herkenhoff, K.E., and Vasavada, A.R., 1999, Dark material in the polar layered deposits and dunes on Mars, *Journal of Geophysical Research*, v. 104, p. 16,487–16,500.
Hofstadter, M.D., and Murray, B.C., 1990, Ice sublimation and topography: Implications for the martian polar layered deposits, *Iceans*, v. 84, p. 352–361.
Howard, A.D., Cuts, J.A., and Blasius, K.R., 1982, Stratigraphic relationships within martian polar cap deposits, *Iceans*, v. 50, p. 161–215.

James, P.B., Briggs, G.E., Barnes, Jeffrey, and Spruck, Andrea, 1979, Seasonal recession of Mars' south polar ice cap as seen by Viking imagery, v. 68, p. 422–461.
Kieffer, H.H., 1990, H_2O grain size and the amount of dust in Mars' residual north polar cap, *Journal of Geophysical Research*, v. 95, no. B2, p. 1481–1493.
Kieffer, H.H., Chase, S.C., Jr., Martin, T.Z., Miner, E.D., and Pallacini, F.D., 1976, Martian north polar summer temperatures: Dirty water ice, *Science*, v. 194, p. 1341–1344.
Malin, M.C., and Edgett, K.S., 2001, Mars Global Surveyor Mars Orbiter Camera—Interpreting craters through time, *Journal of Geophysical Research*, v. 106, p. 23,429–23,570.
Murray, B.C., Soderholm, L.A., Cuts, J.A., Sharp, R.F., Milon, D.J., and Leighton, B.H., 1972, Geological framework of the north polar region of Mars, *Iceans*, v. 17, p. 328–345.
Platt, J.J., Kain, Ralph, Guinness, E.A., and Arvidson, R.E., 1988, Accumulation of sedimentary debris in the south polar region of Mars and implications for climate history, *Iceans*, v. 76, p. 357–377.
Pollack, J.B., and Toon, O.B., 1982, Quasi-periodic climate changes on Mars: A review, *Iceans*, v. 50, p. 259–287.

Scott, D.H., and Carr, M.H., 1978, Geologic map of Mars, U.S. Geological Survey Miscellaneous Investigations Series I-1083, scale 1:250,000.
Smith, D.E., and 18 others, 1999, The global topography of Mars and implications for surface evolution, *Science*, v. 284, p. 1495–1503.
Soderholm, L.A., Malin, M.C., Cuts, J.A., and Murray, B.C., 1973, Mariner 9 observations of the surface of Mars in the north polar region, *Journal of Geophysical Research*, v. 78, p. 4197–4210.
Squires, S.W., 1979, The evolution of dust deposits in the martian north polar region, *Iceans*, v. 40, p. 244–261.
Storrs, A.D., Fanale, F.B., Wadsworth, R.S., and Stephens, J.B., 1988, The formation of filamentary sublimation residues (FSR) from mineral grains, *Iceans*, v. 76, p. 493–512.
Tanaka, K.L., and Scott, D.H., 1987, Geologic map of the polar regions of Mars: U.S. Geological Survey Miscellaneous Investigations Series I-1802-C, scale 1:500,000.

Thomas, Peter, Squires, Steven, Herkenhoff, Ken, Howard, Alan, and Murray, Bruce, 1992, Polar deposits on Mars, in Kieffer, H.H., Jansky, B.M., Snyder, C.W., and Matthews, M.S., eds., *Mars: Tucson, University of Arizona Press*, p. 767–795.
Thomas, P.C., and Weitz, Catherine, 1989, Sand dune materials and polar layered deposits on Mars, *Iceans*, v. 81, p. 185–215.
Toon, O.B., Pollack, J.B., Wood, William, Burns, J.A., and Bökki, Kenneth, 1980, The astronomical theory of climatic change on Mars, *Iceans*, v. 44, p. 552–607.
U.S. Geological Survey, 1966, MTM 85000 controlled photomosaic of part of the Chasma Boreale region of Mars, U.S. Geological Survey Miscellaneous Investigations Series I-1837, two sheets, scale 1:500,000.

Zuber, M.T., and 10 others, 1998, Observations of the north polar region of Mars from the Mars Orbiter Laser Altimeter, *Science*, v. 282, p. 2053–2060.

GEOLOGIC MAP OF THE MTM 85080 QUADRANGLE, CHASMA BOREALE REGION OF MARS

By
Ken Herkenhoff
2003